RMIT
UNIVERSITY

Thank you for downloading this document from the RMIT Research Repository.

The RMIT Research Repository is an open access database showcasing the research outputs of RMIT University researchers.

RMIT Research Repository: http://researchbank.rmit.edu.au/

PLEASE DO NOT REMOVE THIS PAGE

An Innovative Navigation and Guidance System for Small Unmanned Aircraft using Low-Cost Sensors

Roberto Sabatini, Francesco Cappello, Subramanian Ramasamy,

Alessandro Gardi and Reece Clothier

School of Aerospace, Mechanical and Manufacturing Engineering

RMIT University, Melbourne, VIC 3000, Australia

roberto.sabatini@rmit.edu.au

Abstract

Two multi-sensor architectures for navigation and guidance of small Unmanned Aircraft (UA) are proposed and compared in this paper. These architectures are based respectively on a standard Extended Kalman Filter (EKF) approach and a more advanced Unscented Kalman Filter (UKF) approach for data fusion of Global Navigation Satellite Systems (GNSS), Micro-Electro-Mechanical System (MEMS) based Inertial Measurement Unit (IMU) and Vision Based Navigation (VBN) sensors. The main objective is to design a compact, light and relatively inexpensive system capable of providing the Required Navigation Performance (RNP) in all phases of flight of small UA, with a special focus on precision approach and landing. The novelty of this paper is the augmentation of Aircraft Dynamics Model (ADM) in both architectures to compensate for the MEMS-IMU sensor shortcomings in high-dynamics attitude determination tasks. Additionally, the ADM measurements are pre-filtered by an UKF with the purpose of increasing the ADM attitude solution stability time in the UKF based system. After introducing the key mathematical models describing the two architectures, the EKF based VBN-IMU-GNSS-ADM (VIGA) system and the UKF based system (VIGA$^+$) performances are compared in a small UA integration scheme (i.e., AEROSONDE UA platform) exploring a representative cross-section of this UA operational flight envelope, including high dynamics manoeuvres and CAT-I to CAT-III precision approach tasks. The comparison shows that the position and attitude accuracy of the proposed VIGA and VIGA$^+$ systems are compatible with the Required Navigation Performance (RNP) specified in the various UA flight profiles, including precision approach down to CAT-II.

Keywords Aircraft Dynamics Models, Extended/Unscented Kalman Filter, Low-Cost Sensors, Required Navigation Performance, Unmanned Aircraft and Vision Based Navigation.

Paper type Research paper

Introduction

Unmanned Aircraft (UA) are being proposed as alternatives to manned aircraft in an increasing number of civil and military applications. In particular, small UA have the ability of performing tasks with higher manoeuvrability and longer endurance and, additionally, they pose less risk to human lives and nature (Laliberte et al., 2007). For integrating UA into the current and near future non-segregated airspace, they will likely require enhanced navigational capabilities in order to meet the Required Navigational Performance (RNP) and Reduced Vertical Separation Minima (RVSM) expected of manned aircraft (DeGarmo, 2004). Most UA mission- and safety-critical tasks depend on the employment of a variety of sensors, as well as multi-sensor data fusion architectures, to cope with the requirements of long/medium range navigation and landing (including compensating for individual sensors shortcomings) and to provide autonomy to the platform. This approach allows a reduction of cost, weight/volume and support requirements and, with the appropriate combination of sensors and integration algorithms, gives increased accuracy and integrity to the overall system (Sabatini et al., 2012). In this paper, we propose an integrated Navigation and Guidance System (NGS) approach employing two state-of-the-art physical sensors: Micro-Electro-Mechanical System (MEMS)-based Inertial Measurement Unit (IMU) and Global Navigation Satellite Systems (GNSS), as well as augmentation from Aircraft Dynamics Model (ADM) (Bruggemann, 2009), which acts as a virtual sensor. Vision Based Navigation (VBN) sensors are also used for precision approach and landing (i.e., the most demanding and potentially safety-critical flight phase). Our previous research activities (Sabatini et al., 2012) (Sabatini et al., 2013) (Sabatini et al., 2014) presented the various sensor choices, data fusion methods and the overall implementation of the VIG/ADM (VIGA) NGS architecture. MEMS-IMUs are low-cost and low-volume/weight sensors particularly well suited for small/medium size UA applications. However, their integration represents a challenge, which is addressed either by finding improvements to the existing analytical methods or by developing novel algorithmic approaches that counterbalance the use of less accurate inertial sensors. Several VBN sensors and techniques have been developed (Olivares-Mendez et al., 2010) and the vast majority of the VBN sensor schemes fall into Model-based Approach (MBA) and Appearance-based Approach (ABA). The ABA approach was selected for the design and implementation of our VBN sensor system, since it is straightforward to implement the ABA approach compared to 3D modelling. Additionally, the novelty is that the ADM is also used to compensate for the MEMS IMU sensor shortcomings experienced in high-dynamics attitude determination tasks. The ADM Virtual Sensor is essentially a Knowledge-Based Module (KBM), which is used to augment the navigation state vector by predicting the UA flight dynamics (aircraft trajectory and attitude motion). The ADM can employ either a three-degree-of-freedom (3-DoF) or a six-degree-of-freedom (6-DoF) variable mass model with suitable controls and constraints applied in the different phases of flight. The performances achieved by the proposed integrated navigation systems are evaluated against the RNP levels for different phases of flight including take off, climb, cruise, precision approach and landing. Additional research is currently being

carried out on GNSS Carrier Phase Measurements (CFM) for attitude estimation (Sabatini et al., 2013) (Park and Kee, 2006).

Mathematical Model

With respect to the VBN sensor, let (u, v) be the coordinates of a point P defined in the camera frame. The angular rates of the UA are derived using optical flow of the horizon. Optical flow is determined for all the points on the detected horizon line in the images using the classical optical flow equations given by (Sabatini et al., 2012):

$$\begin{bmatrix} \dot{u} \\ \dot{v} \end{bmatrix} = \begin{bmatrix} \frac{uv}{f} & -(f + \frac{u^2}{f}) & v \\ (f + \frac{v^2}{f}) & -\frac{uv}{f} & -u \end{bmatrix} \begin{bmatrix} \omega_x \\ \omega_y \\ \omega_z \end{bmatrix} \tag{1}$$

where f is the focal length and ω is the angular velocity. It was observed that the image processing frontend was susceptible to false detection of the horizon, if any other strong edges were present in the image. Therefore, an Extended Kalman Filter (EKF) is implemented to filter out these incorrect results to provide best estimates of position, velocity and attitude. It is assumed that the motion model of the aircraft is disturbed by uncorrelated zero-mean Gaussian noise. The EKF measurement model is defined as:

$$z_k = H_k * x_k + v_k \tag{2}$$

where z_k is the measurement vector, H_k is the design matrix, x_k is the state vector, v_k is the measurement noise and k is the kth epoch of time, t_k.

$$x_{k+1} = \Phi_k * x_k + G_k * w_k \tag{3}$$

where x_{k+1} is the state vector at epoch $k+1$, Φ_k is the state transition matrix from epoch k to $k+1$, G_k is the shaping matrix and w_k is the process noise. If the body rates are assumed to be constant during the sampling interval, Δt and first order and higher order integrations are applied, then the state transition equations are as follows (Sabatini et al., 2014):

$$\begin{bmatrix} \phi(k+1) \\ \theta(k+1) \\ \omega_x(k+1) \\ \omega_y(k+1) \\ \omega_z(k+1) \end{bmatrix} = \begin{bmatrix} \phi(k) + \Delta t(\dot{\phi}(k)) \\ \theta(k) + \Delta t(\dot{\theta}(k)) \\ \omega_x(k) \\ \omega_y(k) \\ \omega_z(k) \end{bmatrix} + \begin{bmatrix} \eta_\phi(k) \\ \eta_\theta(k) \\ \eta_{\omega_x}(k) \\ \eta_{\omega_y}(k) \\ \eta_{\omega_z}(k) \end{bmatrix} \tag{4}$$

where:

$$\dot{\phi}(k) = (\omega_x(k) \sin(\phi(k)) + \omega_y(k) \cos(\phi(k)) \tan(\phi(k)) + \omega_z(k) \tag{5}$$

$$\dot{\theta}(k) = \omega_x(k) \cos(\phi(k)) - \omega_y(k) \sin(\phi(k)) \tag{6}$$

where θ is the pitch angle and ϕ is the roll angle. The measurement equations are comprised of direct observations of the pitch and the roll measurements from the horizon and i optical flow observations on the detected horizon line. Therefore, the length of the measurement vector $z(k)$ is $2(i + 1)$. The prediction algorithm of the EKF estimates the state vector and

computes the corresponding covariance matrix P_k from the current epoch to the next one using the state transition matrix characterizing the process model described by:

$$P_{k+1}^- = \Phi_{k+1} P_k^+ \Phi_{k+1}^T + Q_k \tag{7}$$

where P_{k+1}^- represents a predicted value computed by the prediction equations and P_k^+ represents the updated values obtained after the correction equations. The process noise at a certain epoch k is characterized by the covariance matrix, Q_k. The updating equations correct the predicted state vector and the corresponding covariance matrix using the measurement model as follows:

$$x_{k+1}^+ = K_{k+1} u_{k+1} \tag{8}$$

$$P_{k+1}^+ = P_{k+1}^- - K_{k+1} H_{k+1} P_{k+1}^- \tag{9}$$

where K_{k+1} is the Kalman gain matrix at epoch, $k+1$ and u_{k+1} is the innovation vector at epoch, $k+1$. The innovation vector represents the difference between the current measurement and the predicted measurement and is given by:

$$u_{k+1} = z_{k+1} - H_{k+1} x_{k+1}^- \tag{10}$$

The Kalman gain is used to quantify the influence of new information present in the innovation vector on the estimation of the state vector and can be considered as a weight factor. It is basically equal to the ratio of the uncertainty on the current measurement and the uncertainty on the predicted one. This gain is defined by (Sabatini et al., 2014):

$$K_{k+1} = P_{k+1}^- H_{k+1}^T [H_{k+1} P_{k+1}^- H_{k+1}^T + R_{k+1}]^{-1} \tag{11}$$

where R_{k+1} is the measurement noise covariance matrix. An Unscented Kalman Filter (UKF) is implemented to increase the accuracy of the measurements and it also aids in pre-filtering the ADM measurements. The UKF is a recursive estimator and is based on unscented transformations in which unscented transforms are used for calculating the statistics of a random variable that goes through a nonlinear transformation. The process model of the UKF is based upon a set of sigma points. The sigma points, χ_i are selected based on the mean and covariance of x_k. The sigma points are calculated using:

$$S_{k-1} = \{chol(P_{k-1})\}^T \tag{12}$$

$$X_{k-1} = \{\hat{x}_{k-1} \ \hat{x}_{k-1} + \gamma S_{k-1} \ \hat{x}_{k-1} - \gamma S_{k-1}\} \tag{13}$$

where P is the lower triangular matrix of the Cholesky factorisation S and γ is the control parameter of the dispersion distance from the mean estimate in the computation of the sigma point matrix X. After the sigma points are calculated, time update is preformed given by:

$$X_{k|k-1}^* = f_d(X_{k-1}, u_{k-1}) \tag{14}$$

$$\hat{x}_k^- = \sum_{i=0}^{2n} w_i X_{i,k|k-1}^* \tag{15}$$

$$P_k^- = \sum_{i=0}^{2n} w_i \left(X_{i,k|k-1}^* - \hat{x}_k^-\right)\left(X_{i,k|k-1}^* - \hat{x}_k^-\right)^T \tag{16}$$

The measurement update equations are given by:

$$K = P_{x_k y_k} P_{\tilde{y}_k \tilde{y}_k}^{-1} \tag{17}$$

$$\hat{x}_k = \hat{x}_k^- + K(y_k - \hat{y}_k^-) \tag{18}$$

$$P_k = P_k^- - K P_{\tilde{y}_k \tilde{y}_k} \mathcal{K}^T \tag{19}$$

$$P_k^- = \sum_{i=0}^{2n} w_i \left(y_{i,k|k-1}^* - \hat{y}_k^-\right)\left(y_{i,k|k-1}^* - \hat{y}_k^-\right)^T \tag{20}$$

where y is the nonlinear function used for propagation of the sigma points. With reference to the implementation of the ADM, six degree of freedom (6-DOF) geodetic nonlinear equations of motion in scalar form are used:

$$\dot{P}_N = (cos\Theta cos\Psi)u + (-cos\Phi sin\Psi + sin\Phi sin\Theta cos\Psi)v + (sin\Phi sin\Psi + cos\Phi sin\Theta cos\Psi)w \tag{21}$$

$$\dot{P}_E = (cos\Theta sin\Psi)u + (cos\Phi cos\Psi + sin\Phi sin\Theta sin\Psi)v + (-sin\Phi sin\Psi + cos\Phi sin\Theta cos\Psi)w \tag{22}$$

$$\dot{h} = (-sin\Theta)u + (sin\Phi cos\Theta)v + (cos\Phi cos\Theta)w \tag{23}$$

$$\dot{u} = (X/m) - gsin\Theta + rv - qw \tag{24}$$

$$\dot{v} = (Y/m) + gsin\phi cos\Theta - ru + pw \tag{25}$$

$$\dot{w} = (Z/m) + gcos\Phi cos\Theta + qu - pv \tag{26}$$

$$\dot{\Phi} = p + qsin\Phi tan\Theta + rcos\Phi tan\Theta \tag{27}$$

$$\dot{\Theta} = qcos\Phi - rsin\Phi \tag{28}$$

$$\dot{\Psi} = qsin\Phi sec\Theta + rcos\Phi sec\Theta \tag{29}$$

where P_N and P_E are the latitude and longitude positions, h is the altitude, g is the gravity acceleration, ϕ is the bank or roll angle, ψ is the yaw or heading angle, Φ is the geodetic latitude, Θ is the geodetic longitude, p is the roll rate, q is the pitch rate, r is the yaw rate, u is the axial velocity, v is the lateral velocity and w is the normal velocity. The overall assumptions associated with the ADM are a rigid body UA, rigidly mounted aircraft engine on the vehicle body, the aircraft mass located in the aircraft centre of gravity and hence the mass is varying only as a result of fuel consumption, neglecting the wind effects, no sideslip, uniform gravity and the geodetic coordinate system of reference is World Geodetic System of year 1984 (WGS 84). The uncertainties in the aerodynamic parameters the primary source of errors in the model resulting from the use of the ADM. The accuracy of these parameters depends on the source of the data, which are theoretical computations, wind tunnel experiments and flight tests. The aerodynamic parameters can also be estimated using an adaptive UKF (Majeed and Kar, 2013). To alleviate the effect of uncertainties, accurate data is used for modelling purposes. The covariance matrix describes the effect of uncertainties in the estimation of the states as a function of time.

VIGA and VIGA[+] Architectures

The two multi-sensor architectures for navigation and guidance integrated navigation system are the VBN-IMU-GNSS-ADM (VIGA) and the VIGA PLUS (VIGA[+]) NGS systems. The VIGA architecture (Sabatini et al., 2014) uses VBN at 20 Hz and Global Positioning System (GPS) at 1 Hz to augment the MEMS-IMU running at 100 Hz. The VIGA architecture is illustrated in Figure 1. This architecture includes the ADM (computations performed at 100 Hz) to provide attitude channel augmentation. The sensor measurements are processed by a sensor processing and data sorting block. The data sorting algorithm is based on Boolean decision logic, which accepts 0 and 1 as input states and allows automatic selection of the sensor data based on pre-defined priority criteria. The sorted data is then fed to an EKF to obtain the best estimate values. The INS position and velocity are compared with the GPS position and velocity to form the measurement input of the data fusion block containing the EKF. The INS and VBN attitude angles differences are incorporated in the EKF measurement vector. The attitude data provided by the ADM and the INS are compared to feed the EKF at 100 Hz, and the attitude data provided by the VBN sensors and INS are compared at 20 Hz and form the inputs to the EKF. The EKF provides estimates of the Position, Velocity and Attitude (PVA) errors, which are then removed from the sensor measurements to obtain the corrected PVA states.

Figure 1   VIGA system.
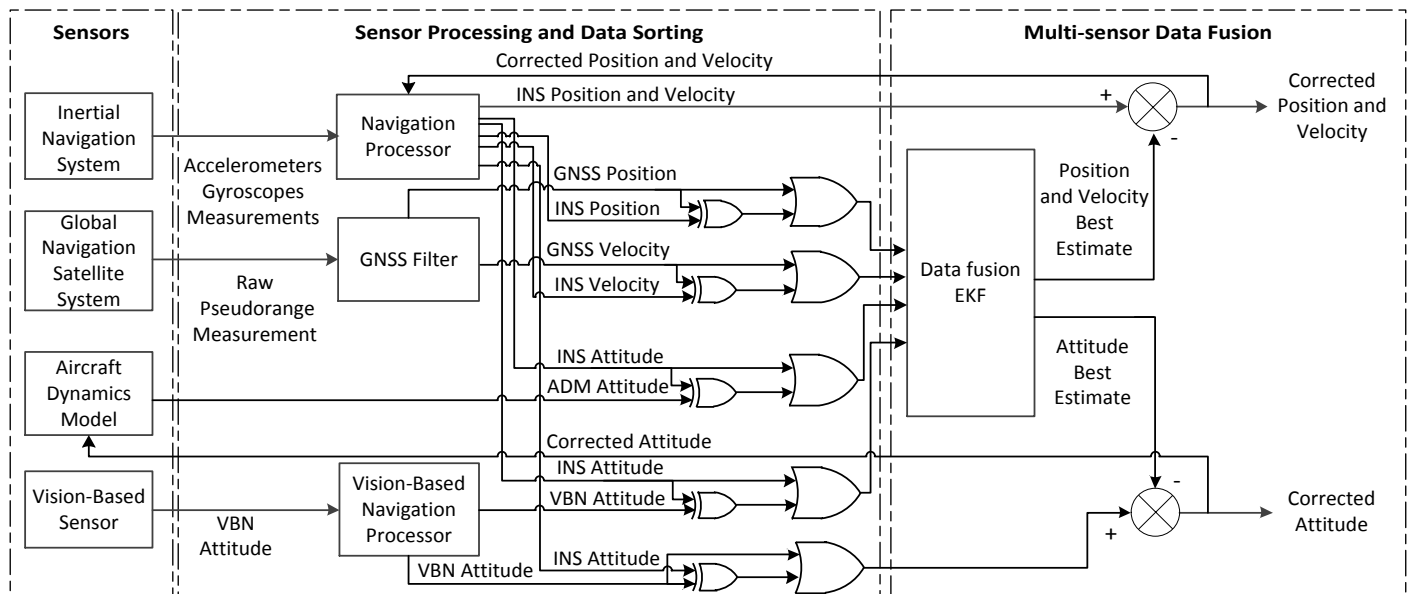
The VIGA[+] architecture is illustrated in Figure 2. In this architecture, the EKF is replaced by an UKF. Additionally, an UKF is also used to pre-process the ADM navigation solution. The ADM operates differently to that of the VIGA system running in parallel to the centralised UKF and acts as a separate subsystem. The pre-filtering of the ADM virtual sensor measurements aids in achieving reduction of the overall position and attitude error budget and importantly considerable reduction in the ADM reinitialisation time. PVA measurements are obtained as state vectors from both the centralised UKF

and ADM/UKF. These measurements are then fed into an error analysis module in which the measurement values of the two UKFs are compared. The error analysis block includes the primary sensors (GNSS, INS and VBN) and it is used to compare the VIG error values with the virtual sensor (ADM) error values to obtain the corrected PVA states.

Figure 2   VIGA$^+$ system.
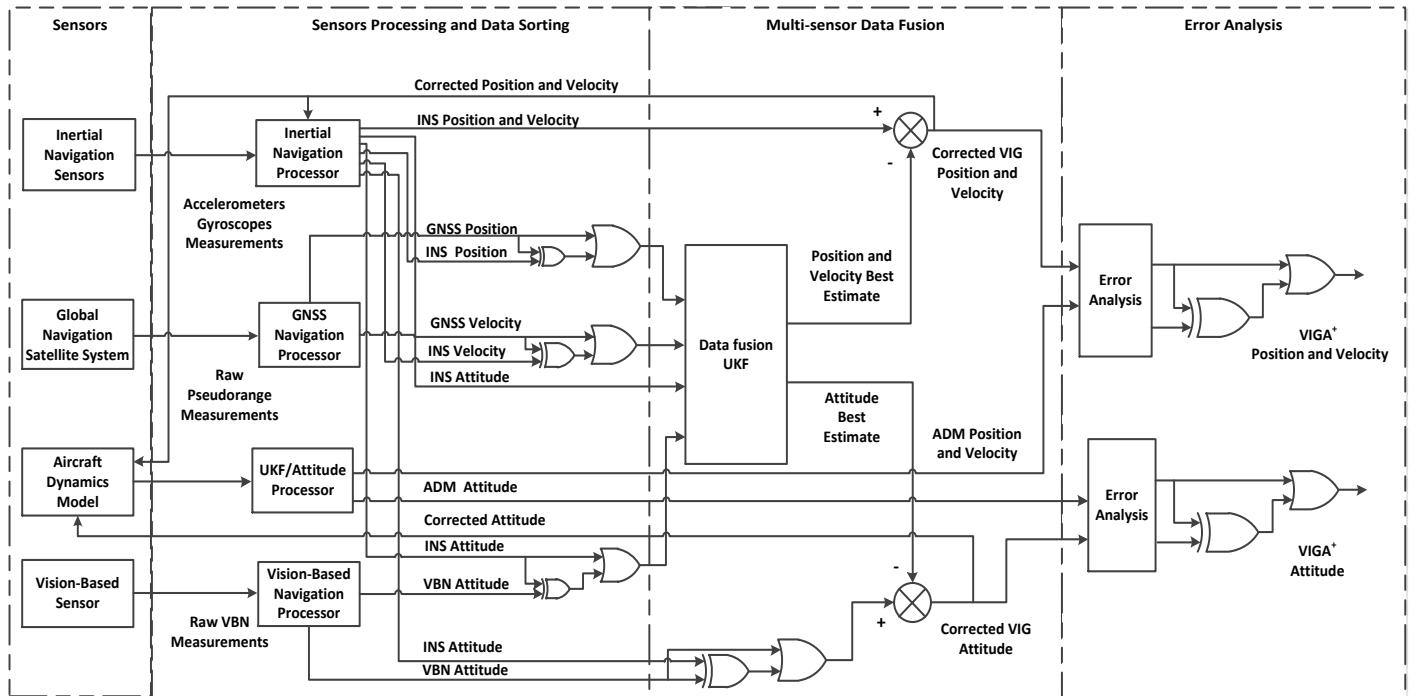
Simulation Results

A detailed case study is performed in a high dynamics UA environment, employing the 6-DoF model of the AEROSONDE UA as the reference ADM. The corresponding VIGA and VIGA$^+$ integrated navigation modes are simulated using MATLAB^{TM} covering all the relevant flight profiles of the UA such as straight climb, straight-and-level flight, level turn, climb/descend turn, straight descent, etc. The VIGA and VIGA$^+$ multi-sensor architectures are tested by simulation in an appropriate sequence of flight manoeuvres representative of the AEROSONDE UA operational flight envelope. The duration of the simulation is 950 seconds covering seven flight legs (i.e., take off, straight climb, climb helix, straight and level cruise, turning descent, curved approach and final straight approach) from starting point to destination. The 3D trajectory plot of the flight profiles of the AEROSONDE UA is illustrated in Figure 3.

Figure 3   3D trajectory plot of UA flight profile.
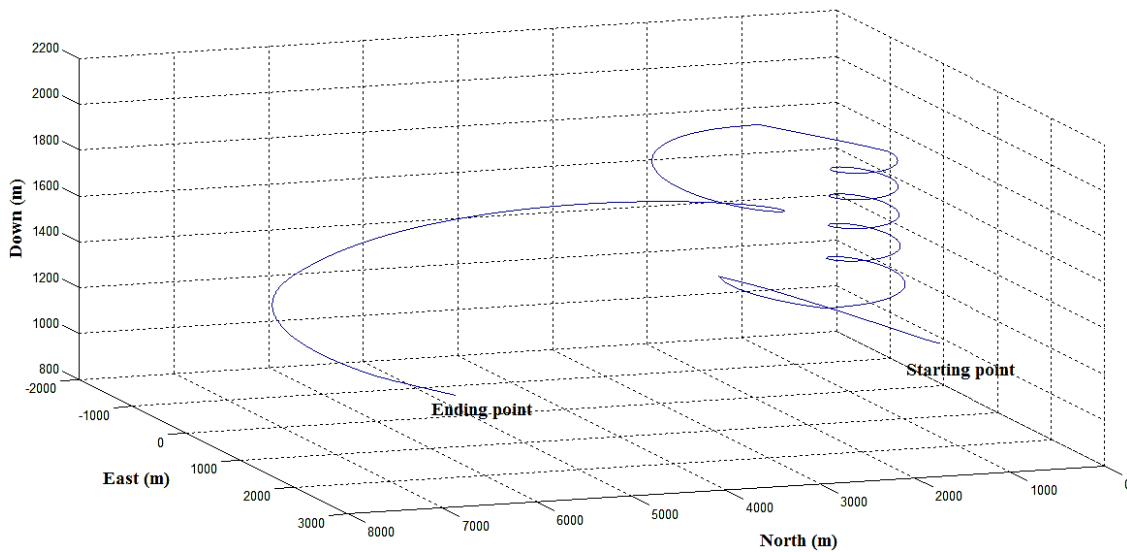
The position, velocity and attitude best estimates of the two NGS architectures are obtained and the associated error statistics (mean, μ and standard deviation, σ) are calculated. Tables 1 and 2 list the position and attitude error statistics of the two NGS architectures respectively. The VIGA NGS system is prone to rapid divergence and its optimal time for reinitialisation is in the order of 20 seconds. The VIGA$^+$ NGS system shows considerable improvement in the horizontal and vertical positions. Additionally, the VIGA$^+$ system demonstrates promising results in the performance of the modified ADM. By applying an UKF to pre filter the ADM measurements, the navigational solution is corrected and it is useful for an extended period of operation. Comparing with the VIGA solution, a significant improvement of the solution validity time is obtained with the VIGA$^+$ system as shown in Table 3. In particular, the validity time before the solution exceeds the RNP 1 threshold in the climb phase is 76 sec and, in the final approach phase, the ADM solution exceeds the CAT I, CAT II and CAT III limits at 53 sec, 30 sec and 20 sec respectively (the VIGA was compliant with CAT I up to 34 sec, CAT II up to 19 sec and CAT III up to sec to 16 sec). The vertical channel was found to satisfy CAT III and CAT II requirements up to 100 sec and CAT I requirements up to 365 sec. Table 4 lists a comparison of the VIGA and VIGA$^+$ horizontal and vertical accuracy (RMS-95%) with the required accuracy levels for precision approach as recommended by the International Civil Aviation Organization (ICAO) (CAA, 2003) (ICAO, 2006) and the obtained results are in line with CAT II precision approach requirements.

Table 1   Position error statistics.

NGS Architecture	North Position [m]		East Position [m]		Down Position [m]	
	μ	σ	μ	σ	μ	σ
VIGA	0.3652	1.9028	-0.4849	1.9435	0.1674	2.4411
VIGA$^+$	0.4793	1.4062	-0.4064	1.7339	0.1211	2.2581

Table 2 Attitude error statistics.

NGS Architecture	Pitch (θ) [degrees]		Roll (ϕ) [degrees]		Heading (ψ) [degrees]	
	μ	σ	μ	σ	μ	σ
VIGA	0.0052	0.0406	-0.0065	0.3138	-0.0011	0.0447
VIGA$^+$	0.0051	0.0400	-0.0053	0.2197	0.0010	0.0417

Table 3 VIGA and VIGA$^+$ ADM lateral guidance validity time.

Accuracy threshold	ADM validity time [sec]	
	VIGA	VIGA$^+$
RNP 1	65	76
CAT I	34	56
CAT II	19	30
CAT III	16	20

Table 4 VIGA and VIGA$^+$ position error statistics (precision approach).

Category of approach	Horizontal Accuracy (m) 2D RMS - 95%			Vertical Accuracy (m) RMS - 95% Down		
	Required	VIGA	VIGA$^+$	Required	VIGA	VIGA$^+$
CAT I	16			4		
CAT II	6.9	5.2	4.8	2	1.9	1.9
CAT III	4.1			2		

Conclusion

The research activities performed to design a low-cost and low-weight/volume integrated Navigation and Guidance System (NGS) suitable for small size UA applications were described. Various sensors were considered for the design of the NGS. GNSS and MEMS-IMUs, with augmentation from ADM and VBN sensors, were selected for integration. Two different low-cost and low-weight/volume integrated Navigation and Guidance System (NGS) architectures were introduced. They are an EKF based VBN-IMU-GNSS-ADM (VIGA) integrated system and an UKF based (VIGA$^+$) system. While the VIGA system uses unfiltered ADM data, the VIGA$^+$ system employs an UKF for pre-filtering the ADM attitude solution, so to increase the ADM attitude solution stability (validity time of 65 sec before exceeding the RNP thresholds). Simulation of the VIGA integrated navigation mode showed that the integration schemes can achieve horizontal/vertical position accuracies, with a significant improvement compared to stand-alone GNSS and integrated GNSS/INS. Compared to the VIGA system, the VIGA$^+$ system showed an improvement of accuracy in the position and attitude measurements in addition to an increased ADM stability time. Furthermore, the integration schemes achieved horizontal/vertical position accuracies in line with precision approach and landing requirements.

Further Work

Future research will address the uncertainty analysis and possible synergies of the VIGA and VIGA$^+$ architectures with GNSS space, ground and avionics based integrity augmentation systems (Sabatini et al., 2013 b). The integrated navigation and guidance systems are currently adopted for use in other UA platforms including the JAVELIN UA (Burston et al., 2014).

References

Bruggemann, T.S. (2009), "Investigation of MEMS Inertial Sensors and Aircraft Dynamic Models in Global Positioning System Integrity Monitoring for Approaches with Vertical Guidance", PhD Thesis, Queensland University of Technology, Australia.

Burston, M., Sabatini, R., Gardi, A. and Clothier, R. (2014), "Reverse Engineering of a Fixed Wing Unmanned Aircraft 6-DoF Model Based on Laser Scanner Measurements", *IEEE Metrology for Aerospace Conference 2014*, Benevento, Italy.

CAA, (2003), "Safety Regulation Group Paper 2003/09", GPS Integrity and Potential Impact on Aviation Safety.

DeGarmo, M.T. (2004), "Issues Concerning Integration of Unmanned Aerial Vehicles in Civil Airspace", *MITRE*.

ICAO, (2006), "Annex 10 to the Convention on International Civil Aviation, Aeronautical Telecommunications - Volume 1: Radio Navigation Aids", Edition 6.

Laliberte, A.S., Rango, A. and Herrick, J.E. (2007), "Unmanned aerial vehicles for rangeland mapping and monitoring: A comparison of two systems", *Proceedings of the ASPRS Annual Conference*, Tampa, FL, USA.

Majeed, M. and Kar, I.N. (2013), "Aerodynamic parameter estimation using adaptive unscented Kalman filter", *Aircraft Engineering and Aerospace Technology*, Vol. 85 No. 4, pp. 267–279. DOI: 10.1108/AEAT-Mar-2011-0038

Olivares-Mendez, M.A., Mondragon, I.F., Campoy, P. and Martinez, C. (2010), "Fuzzy controller for UA-landing task using 3D position visual estimation", *IEEE International Conference on Fuzzy Systems*, Barcelona, Spain.

Park, S. and Kee, C. (2006), "Enhanced method for single-antenna GPS-based attitude determination", *Aircraft Engineering and Aerospace Technology*, Vol. 78 No. 3, pp. 236 – 243. DOI: 10.1108/17488840610663701

Sabatini, R., Rodríguez, L., Kaharkar, A., Bartel C. and Shaid, T. (2012), "Low-Cost Vision Sensors and Integrated Systems for Unmanned Aerial Vehicle Navigation and Guidance", *ARPN Journal of Systems and Software*, ISSN: 2222-9833, Vol. 2 No. 11, pp. 323-349.

Sabatini, R., Rodríguez, L., Kaharkar, A., Bartel C. and Shaid, T. (2012), "Carrier-Phase GNSS Attitude Determination and Control System for Unmanned Aerial Vehicle Applications", *ARPN Journal of Systems and Software*, ISSN: 2222-9833, Vol. 2 No. 11, pp. 297-322.

Sabatini, R., Bartel C., Kaharkar, A., Shaid, T., Rodríguez, L., Zammit-Mangion D. and Jia, H. (2012) "Low-Cost Navigation and Guidance Systems for Unmanned Aerial Vehicles – Part 1: Vision-Based and Integrated Sensors", *Annual of Navigation*, Vol. 19 No.2, pp. 71-98. DOI: 10.2478/v10367-012-0019-3

Sabatini, R., Ramasamy, S., Gardi A. and Rodríguez, L. (2013), "Low-cost Sensors Data Fusion for Small Size Unmanned Aerial Vehicles Navigation and Guidance", *International Journal of Unmanned Systems Engineering*, Vol. 1 No. 3, pp.16-47. DOI: 10.14323/ijuseng.2013.11

Sabatini, R., Rodríguez, L., Kaharkar, A., Bartel C., Shaid, T. and Zammit-Mangion, D. (2013), "Low-Cost Navigation and Guidance Systems for Unmanned Aerial Vehicles – Part 2: Attitude Determination and Control", *Annual of Navigation*, Vol. 20, pp. 97-126. DOI: 10.2478/aon-2013-0008

Sabatini, R., Kaharkar, A., Bartel C. and Shaid, T. (2013), "Carrier-phase GNSS Attitude Determination and Control for Small UA Applications", *Journal of Aeronautics and Aerospace Engineering*, Vol. 2 No. 4. DOI: 10.4172/2168-9792.1000120

Sabatini, R., Richardson M.A., Bartel C., Shaid, T. and Ramasamy, S. (2013), "A Low-cost Vision Based Navigation System for Small Size Unmanned Aerial Vehicle Applications", *Journal of Aeronautics and Aerospace Engineering*, Vol. 2 No. 3. DOI: 10.4172/2168-9792.1000110

Sabatini, R., Moore, T. and Hill, C. (2013 b), "A Novel GNSS Integrity Augmentation System for Civil and Military Aircraft", *International Journal of Mechanical, Industrial Science and Engineering*, Vol. 7 No. 12, pp. 1433-1449.

Sabatini, R., Moore, T. and Hill, C. (2013 b), "A New Avionics-Based GNSS Integrity Augmentation System: Part 1 – Fundamentals", *Journal of Navigation*, Vol. 66 No. 3, pp. 363–384. DOI: 10.1017/S0373463313000027

Sabatini, R., Moore, T. and Hill, C. (2013 b), "A New Avionics-Based GNSS Integrity Augmentation System: Part 2 – Integrity Flags", *Journal of Navigation*, Vol. 66 No. 4, pp. 501–522, DOI: 10.1017/S0373463313000143

Sabatini, R., Bartel C., Kaharkar, A., Shaid, T. and Ramasamy S. (2014), "Navigation and Guidance System Architectures for Small Unmanned Aircraft Applications", *International Journal of Mechanical, Industrial Science and Engineering*, Vol. 8 No. 4, pp. 733-752.